2017-09-06

Baffin Bay paleoenvironments in the LGM and HS1: Resolving the ice-shelf question

Jennings, AE

10.1016/j.margeo.2017.09.002
Marine Geology
Elsevier

Baffin Bay Paleoenvironments in the LGM and HS1: Resolving the ice-shelf question

Anne E. Jennings[1*], John T. Andrews[1], Colm Ó Cofaigh[2], Guillaume St-Onge[3], Simon Belt[4], Patricia Cabedo-Sanz[4], Christof Pearce[5,6],Claude Hillaire-Marcel[7], D. Calvin Campbell[8]

[1] INSTAAR University of Colorado, Campus Box 450, Boulder, CO 80309-0450 USA

[2] Department of Geography, Durham University, South Road, Durham DH1 3LE, United Kingdom

[3] Institut des sciences de la mer de Rimouski (ISMER) Université du Québec à Rimouski and GEOTOP Rimouski, Québec, Canada S5L 3A1

[4] School of Geography, Earth and Environmental Sciences, University of Plymouth, Plymouth PL4 8AA United Kingdom

[5] Department of Geological Sciences and Bolin Centre for Climate Research, Stockholm University, Svante Arrhenius väg 8, SE-106 91 Stockholm, Sweden

[6] Department of Geoscience and Arctic Research Centre, Aarhus University, Hoegh Guldbergs gade 2, 8000 Aarhus, Denmark

[7] Université du Québec a Montréal, Centre GEOTOP CP 8888, succ. Centre-Ville, Montréal, Québec, Canada, H3C 3P8

[8] Geological Survey of Canada-Atlantic, Natural Resources Canada, Dartmouth Nova Scotia

* anne.jennings@colorado.edu

Core HU2008029-12PC from the Disko trough mouth fan on the central West Greenland continental slope is used to test whether an ice shelf covered Baffin Bay during the Last Glacial Maximum (LGM) and at the onset of the deglaciation. We use benthic and planktic foraminiferal assemblages, stable isotope analysis of planktic forams, algal biomarkers, ice-rafted detritus (IRD), lithofacies characteristics defined from CT scans, and quantitative mineralogy to reconstruct paleoceanographic conditions, sediment processes and sediment provenance. The chronology is based on radiocarbon dates on planktic foraminifers using a ΔR of 140 ± 30 ^{14}C years, supplemented by the varying reservoir estimates of Stern and Lisiecki (2013) that provide an envelope of potential ages. HU2008029-12PC is bioturbated throughout. Sediments between the core base at 11.3 m and 4.6 m (LGM through HS1) comprise thin turbidites, plumites and hemipelagic sediments with Greenlandic provenance consistent with processes active at the Greenland Ice Sheet margin grounded at or near the shelf edge. Abundance spikes of planktic forams coincide with elevated abundance of benthic forams in assemblages indicative of chilled Atlantic Water, meltwater and intermittent marine productivity. IRD and IP_{25} are rare in this interval, but brassicasterol, an indicator of marine productivity reaches and sustains low levels during the LGM. These biological characteristics are consistent with a sea-ice covered ocean experiencing periods of more open water such as leads or polynyas in the sea ice cover, with chilled Atlantic Water at depth, rather than full ice-shelf cover. They do not support the existence of a full Baffin Bay ice shelf cover extending from grounded ice on the Davis Strait. Initial ice retreat from the West Greenland margin is manifested by a pronounced lithofacies shift to bioturbated, diatomaceous mud with rare IRD of Greenlandic origin at 467 cm (16.2 cal ka BP; ΔR=140 yrs) within HS1. A spike in foraminiferal abundance and ocean warmth indicator benthic forams precedes the initial ice retreat from the shelf edge. At the end of HS1, IP_{25}, brassicasterol and benthic

forams indicative of sea-ice edge productivity increase, indicating warming interstadial conditions. Within the Bølling/Allerød interstadial a strong rise in IP_{25} content and IRD spikes rich in detrital carbonate from northern Baffin Bay indicate that northern Baffin Bay ice streams were retreating and provides evidence for increased open water, advection of Atlantic Water in the West Greenland Current, and formation of an IRD belt along the W. Greenland margin.

Keywords: Greenland Ice Sheet, Baffin Bay, paleoceanography, ice shelf, foraminifera, Heinrich Stadial 1

1. Introduction

Last Glacial Maximum (LGM) climatic and oceanic conditions in Baffin Bay are currently poorly known, but according to the temperature reconstructions from the Greenland Ice Sheet borehole (Dahl-Jensen and al., 1998) and ice-core data (Buizert et al., 2014), summit temperatures were ~20°C colder than present. Applying this temperature difference down to sea level using the adiabatic lapse rate, suggests that the annual temperature at the surface of Baffin Bay adjacent to Baffin Island would approach -36°C. Such cold temperatures support the argument that cold-based ice covered the forelands of eastern Baffin Island (Briner et al., 2003) with “Antarctic-like” conditions across Baffin Bay, which would also suggest that Baffin Bay was covered in perennial sea ice. At the LGM, confluent, Innuitian (IIS), Laurentide (LIS) and Greenland (GIS) ice sheets (England et al., 2006) blocked the channels that connect Baffin Bay to the Arctic Ocean (Dyke, 2002) and terminated in northern Baffin Bay as large ice streams (Li et al., 2011; Blake, 1977). The Greenland ice sheet reached the continental shelf edge via large ice streams off west Greenland (Ó Cofaigh et al., 2013a; Jennings et al., 2017; Slabon et al., 2016; Sheldon et al., 2016; Dowdeswell et al., 2014), but the outer limits of the ice on the Baffin shelf are not known.

On the basis of modeling, it has been proposed that Baffin Bay was blocked at its southern end by an ice shelf extension of the Hudson Strait ice stream that grounded across Davis Strait to reach southern Greenland, thus sealing Baffin Bay from the Labrador Sea (Hulbe et al., 1997; Álvarez-Solas et al., 2010; Marcott et al., 2011). This ice shelf was the starting point for modeling the processes that produce Heinrich events (Hulbe et al., 1997; Álvarez-Solas et al., 2010; Marcott et al., 2011), but physical evidence for it has not been recovered. An ice shelf of this scale would have environmental consequences that should be recorded in Baffin Bay sediments. Firstly, grounding of a Labrador Sea ice shelf along Davis Strait would prevent seawater exchange between Baffin Bay and the Labrador Sea, excluding advection of organic matter into Baffin Bay. It also would shut down *in situ* primary marine productivity in Baffin Bay so that planktic and benthic organisms, their biomarkers, and bioturbation would be absent in the sediment. Secondly, ice shelves and even extensive sea-ice cover are known to restrict the movement and export of icebergs (Reeh et al., 2001; Domack and Harris, 1998). Thus iceberg rafting and mixing of sediments of various provenances in Baffin Bay would be reduced. Using these concepts, we test the LGM Baffin Bay ice-shelf hypothesis by studying the sedimentological and biological characteristics of sediments in HU2008029-12PC from the continental slope off western Greenland, a core that extends from the LGM into the Younger Dryas (YD) and that recorded retreat of the Greenland Ice Sheet during deglaciation (Jennings et al., 2017).

2. Setting of core HU2008029-12PC

Detailed studies of LGM and deglacial environments in Baffin Bay have been hampered by relatively slow sediment accumulation rates and poor calcium carbonate preservation (cf. Aksu, 1985; de Vernal et al., 1992; Simon et al., 2012). HU2008029-12PC (hereafter called 12PC) was raised from the northern side of the Disko trough mouth fan (TMF) from acoustically stratified sediments with continuous parallel reflections on the eastern side of Baffin Bay (68°13.69’ N; 57°37.08’ W; 1475 m water depth; Campbell and de Vernal, 2009) (Figs. 1 and 2). This site on the trough mouth fan has higher sediment accumulation than sites in the deep basin of Baffin Bay that have variable sedimentation rates that range between 3 and 35 cm/ka (Andrews et al., 1998; Hillaire-Marcel et al., 1989, 2004; Simon et al., 2012; 2014) (Fig. 1).

The Disko TMF was built throughout the Quaternary by rapid sediment deposition in front of the fast flowing Disko ice stream (Fig. 1) when the GIS margin was extended on the shelf, and from hemipelagic sedimentation during and after ice retreat (ÓCofaigh et al., 2013a, b; Jennings et al., 2017; Hofmann et al., 2016). An ice sheet grounded at or near the shelf edge delivers abundant sediments directly to the continental slope in the form of sediment gravity flows, including turbidity currents that form graded sand layers, stratified sand/silt beds, and glacigenic debris flows (ÓCofaigh et al., 2013a, b, Lucci and Rebesco, 2007). Turbid meltwater plumes released from the ice front produce plumites, which are finer grained than the turbidites as the sand is dropped near the ice front and the silt and clay continue offshore in suspension (Hesse et al., 1997; Lucchi and Rebesco, 2007). Depending on sea surface conditions such as perennial sea ice and/or ice shelves, icebergs would also deliver sediment to the slope as they melted

123 during their transit in Baffin Bay (Andrews et al., 1998; 2014; Jennings et al., 2014;
124 Simon et al., 2012; 2014; 2016; Sheldon et al., 2016).

125 The modern sea ice edge extends southeast to northwest within Baffin Bay and
126 sea ice cover is greater in the western than in the eastern half due to the influence of the
127 relatively warm and saline West Greenland Current that enters Baffin Bay from the
128 southeast (Tang et al., 2004; Münchow et al., 2015) (Fig. 1). The boundary between
129 lower salinity, sea-ice bearing, Arctic Surface Water (ASW) that passes from the Arctic
130 Ocean through the channels of the Canadian Arctic Archipelago into Baffin Bay and
131 Atlantic Waters of the West Greenland Current (WGC) moving northward along West
132 Greenland is oriented NE-SW and migrates through the year. The relatively warm, saline
133 Atlantic Water submerges beneath the ASW (Buch, 2000a, b) and forms the West
134 Greenland Intermediate Water (WGIW) (Fig. 1 inset) (Tang et al., 2004). During the
135 LGM, however, the circulation regime in Baffin Bay would have been different because
136 the southward flow of ASW into Baffin Bay was blocked by confluent ice sheets
137 grounded in the channels of the Canadian Arctic Archipelago until the early Holocene
138 (England, 1999; Zreda et al., 1999; Jennings et al., 2011a; Piénkowski et al., 2011).
139 Today, warm Atlantic Water carried in the WGC accesses the GIS margins via cross
140 shelf troughs and fjords, where the ice sheet terminates in the sea (Holland et al., 2008)
141 and promotes basal melting (Straneo et al., 2012). WGC Atlantic Water flow was
142 initiated as early as 14.4 cal ka BP off central West Greenland and is implicated in
143 Greenland Ice Sheet retreat from the LGM position at the shelf edge (cf. Knutz et al.,
144 2011; Sheldon et al., 2016; Jennings et al., 2017).
145

3. Methods:

3.1 Age Model

The age model for 12PC is based on 7 radiocarbon dates between 201 and 860 cm on the arctic planktic foraminifer, *Neogloboquadrina pachyderma* (*sensu* Darling et al., 2006). The dates were previously published in Jennings et al., (2017) (Table 1). Radiocarbon dates were calibrated using the Marine13 curve (Reimer et al., 2013). OxCal version 4.2.4 (Ramsey and Lee, 2013) was used to compute an age/depth model (Fig. 3). An age reversal in the upper 110 cm of the core limited the chronology to the interval from 200 cm to the base of the core (1130 cm). The age of the core base is assumed to be no older than 26.5 ka BP, the beginning of the LGM (Clark et al., 2009). This assumed basal age results in a large uncertainty in the modeled age of the base of the core (24 to 28 cal ka BP). Given this basal age, we might expect to record Baffin Bay Detrital Carbonate (BBDC) event BBDC3 that is found in central Baffin Bay from c. 23.5 to 25 cal ka BP (Simon et al., 2016). A single data point with 20% NBB source at 21.5 cal ka BP may represent BBDC2 (21 cal ka BP; Simon et al., 2016) although it is not associated with a coarse clast-rich interval as would be expected if it represented a BBDC event (Andrews et al., 1998; Simon et al., 2012; Jackson et al., 2017) (Fig. 3). The lack of an interval of high NBB and IRD below 467 cm (16.2 cal ka BP) in 12PC indicates that BBDC2 and BBDC3 were not recovered in 12PC. Either these two events were not deposited basin wide or the basal age of 12PC is younger than the 21 ka BP age of BBDC2. Given that the deepest radiocarbon age in 12PC is 21.8 cal ka BP (ΔR=140 years) and there are 3 meters of sediment below this depth in the core, we suggest it is more likely that BBDC2 and 3 were not deposited basin wide. Without additional information we continue with

the assumption that the core base is no older than the beginning of the global LGM of 26.5 ka BP (Clark et al., 2009).

We initially built the age model assuming a marine reservoir offset (ΔR) of 140±30 years based on recent work in Disko Bugt (Lloyd et al., 2011), for consistency with other central West Greenland sediment core records (cf Jennings et al., 2014; 2017; Jackson et al., 2017; Hogan et al., 2016; Sheldon et al., 2016), and we note that prior to 2011, many publications used a ΔR=0 years (Andrews et al., 1998; Knudsen et al., 2008). However, recognizing that the marine reservoir offset could be large and variable over the time interval of 12PC and because this core extends into the LGM, defined here as beginning at 26.5 ka (Clark et al., 2009) and ending at the beginning of the Oldest Dryas period, 18 ka BP (Buizert et al., 2014), we used the variable North Atlantic R values in Stern and Lisiecki (2013) to provide an envelope of calibrated age so that we could consider the correlations of boundaries and conditions recorded in the core with established climatic intervals (Fig. 3f). To accomplish this we first calibrated each date with ΔR=0 ^{14}C years, which provides the maximum age. We then used the ΔR=0 ages to identify the appropriate 500 year bin of maximum, average and minimum R values from Table S1 of Stern and Lisiecki (2013) and calibrated each of the dates using these three R-values. The resulting envelope of ages, from ΔR=0 to the maximum Stern and Lisiecki 2013 R-value, illustrates how the choice of ΔR affects correlation of boundaries in the core with climate intervals from LGM through the YD (Fig. 3f; Table 1). Regardless, these results confirm that the core contains LGM and Heinrich Stadial 1 (aka Oldest Dryas) sediments, a key requirement for testing the ice shelf model (Hulbe et al., 1997; Álvarez-Solas et al., 2010; Marcott et al., 2011).

192

193 3.2 Foraminiferal analyses.

194 One-cm wide samples were weighed wet and sieved on a 63-µm screen. Material >63
195 µm was kept wet in a storage solution of 70% distilled water and 30% ethanol with
196 baking soda as a buffer. Foraminifera were counted wet to prevent destruction of fragile
197 tests that disintegrate under the stress of drying. A wet splitter was used when necessary
198 to achieve a count of 200-300 benthic formaminifers and as many planktic foraminifers
199 as were in the benthic split. In most cases the full sample was counted. Equivalent dry
200 weights of the foram samples were estimated from sedimentology samples from the same
201 depths that had both wet and dry weights, allowing foraminifera/gram sediment to be
202 calculated.

203

204 3.3 Stable isotope analyses

205 Stable oxygen and carbon isotopes were measured on the planktic foram species
206 *Neogloboquadrina pachyderma* picked from the 150-250 µm size fraction in 41 samples;
207 results from 3 samples were rejected because they yielded a low signal. Samples >100 µg
208 have standard deviations of 0.01 and 0.03 ‰ for $\delta^{13}C$ and $\delta^{18}O$ respectively. Samples
209 weighing <100 µg are reported with a standard deviation of 0.06 ‰ for $\delta^{13}C$, and an error
210 of ±0.2 ‰ for $\delta^{18}O$. The oxygen isotope values are expressed as ‰ vs VPDB. Between
211 1050 and 857 cm all samples were of small weight but otherwise seemed reliable.
212 Measurements were made on a Micromass IsoprimeTM dual inlet coupled to a
213 MulticarbTM system at the Light Stable Isotope Geochemistry Laboratory at the
214 University of Montréal – UQAM.

215

3.4 CT scan.

CT scanning of the half round core was performed at the sediment core laboratory at the University of Quebec at Rimouski. A CT number (a measure of sediment density) was extracted from the images. The CT scan image was used to determine lithofacies and boundaries, sedimentary structures, and to identify bioturbation, a key source of evidence for the presence of benthic organisms and a source of information about sedimentation rate variations between the radiocarbon dates (Wetzel, 1991). Counts of >2 mm clasts interpreted as ice rafted detritus (IRD) were made from the CT images by counting in a 2 cm wide window across the core width continuously along the core length (Grobe, 1987).

3.5 Biomarkers: IP_{25} and Brassicasterol

Biomarker analyses (IP_{25} and brassicasterol) were performed using methods described previously (Belt et al., 2012; Belt et al., 2015). Briefly, 9-octylheptadec-8-ene (9-OHD, 10 µL; 10 µg mL^{-1}) and 5α-androstan-3β-ol (10 µL; 10 µg mL^{-1}) were added to ca. 1 – 2 g of each freeze-dried sediment sample prior to extraction to permit quantification of IP_{25} and sterols, respectively. Samples were then extracted using dichloromethane/methanol (3 x 3 mL; 2:1 v/v) and ultrasonication. Following removal of the solvent from the combined extracts using nitrogen, the resulting total organic extracts (TOE) were purified using column chromatography (silica) with IP_{25} (hexane; 6 mL) and brassicasterol (20:80 methylacetate/hexane; 6 mL) collected as two single fractions. Non-polar lipid fractions were further separated into saturated and unsaturated hydrocarbons using glass pipettes containing silver ion solid phase extraction material (Supelco Discovery® Ag-Ion). Saturated hydrocarbons were eluted with hexane (1 mL), while unsaturated hydrocarbons

239 (including IP_{25}) were eluted with acetone (2 mL). All fractions were dried under a stream
240 of nitrogen.

241 Analysis of individual fractions was carried out using gas chromatography - mass
242 spectrometry (GC-MS) with operating conditions as described previously (e.g. Belt et al.,
243 2012; Brown and Belt, 2012). Sterols were derivatized (BSTFA; 50 µL; 70 ºC; 1 h) prior
244 to analysis by GC-MS. Mass spectrometric analysis was carried out in total ion current
245 (TIC) and single-ion monitoring (SIM) modes. Individual lipids were identified on the
246 basis of their characteristic GC retention indices and mass spectra obtained from
247 standards. Quantification of IP_{25} was achieved by dividing its integrated GC-MS peak
248 area by that of the internal standard (9-OHD) in SIM mode (both *m/z* 350) and
249 normalizing this ratio using an instrumental response factor (obtained from laboratory
250 standards of each analyte) and the mass of sediment (Belt et al., 2012). Analytical
251 reproducibility (6 %, n = 3) was monitored using a sediment with a known concentration
252 of IP_{25}. Brassicasterol concentrations were obtained by comparison of their respective
253 peak areas in SIM mode (brassicasterol, *m/z* 470) with those of the internal standard (*m/z*
254 333) and normalized as per IP_{25}.
255
256 3.6 Quantitative X-ray diffraction Mineralogy
257 Quantitative x-ray diffraction (qXRD) analyses were used to identify shifts in sediment
258 sources between ‘local’ West Greenland (WG) and ‘distal’ Northern Baffin Bay (NBB).
259 Samples for qXRD analysis were taken at 10 to 20 cm intervals throughout the core.
260 Sediment samples were freeze-dried and processed at INSTAAR using the method
261 described by Eberl (2003) and Andrews and Eberl (2011). The qXRD samples were

analysed on a Siemens D5000 XRD unit at a 0.02 2-θ step with a 2 second count; minerals were identified using the program RockJock v.6 (Eberl, 2003). The qXRD 2-source data to 17.5 cal ka BP is presented in Jennings et al. (2017). The determination of sediment provenance is based on the quantitative X-ray diffraction (qXRD) analysis of the < 2 mm surface and core sediments using the method outlined by Eberl (2003) and described in more detail for our area by (Andrews and Eberl, 2012; Andrews et al., 2014; O'Cofaigh et al., 2013a; Simon et al., 2014). We use the Excel macro unmixing program “SedUnMix” (Eberl, 2004; Andrews and Eberl, 2012) to ascribe sediment mineral assemblages to probable source areas. In this present study we discriminated between two glacial derived sources; first a regional West Greenland source dominated by specific ranges in quartz, plagioclase, k-feldspars and other non-clay and clay minerals, versus a North Baffin Bay detrital carbonate source dominated by dolomite (Andrews et al., 2014; O'Cofaigh et al., 2013; Jennings et al., 2017).

4. Results and Interpretation

4.1 Lithofacies Characteristics

There are two main lithofacies units defined by the sediment parameters in 12PC (Fig. 3). The boundary between the two units (Fig. 4b) is well expressed by an abrupt shift to lower CT# (Fig. 3A). This transition dates to 16.2 cal ka BP using ΔR=140 years and has been interpreted to represent the retreat of the Greenland Ice Sheet from the shelf edge (Jennings et al., 2017). However, the full age-envelope ranges between 16.4 (ΔR=0) to 14.0 (Max R) ka, or, late in Heinrich Stadial 1 to the end of the Bølling (Fig. 3f). Calibrated radiocarbon dates (Fig. 3F; ΔR=140, pink) in the lower unit range from

21.8 to 16.2 cal ka BP. The lower three radiocarbon dates fall within the LGM regardless of the marine reservoir age selected (Fig. 3F). The radiocarbon date at 571.5 cm falls within Heinrich Stadial 1 regardless of the marine reservoir age (Fig. 3F).

The lower lithofacies unit, which represents the period when the ice sheet grounding line was at or near the shelf edge, has higher magnetic susceptibility (Fig. 3C), variable sand content including high weight percentage peaks (Fig. 3D) and a west Greenlandic sediment composition (Fig. 3E) but rare >2mm clasts (Fig. 3B). From the base of the core to 1022 cm, sediments are laminated mud with straight, sharp contacts defining the laminae and vertically oriented burrows (Fig. 4f). Between 1025 and 768 cm the sand content increases and stratification is disrupted by bioturbation (Fig. 3E). Stratified mud with distinct vertical burrows extends from 768 to 735 cm (Fig. 3D). From 735 cm to 688 cm sand content increases. This sandy unit is overlain by another sequence of stratified mud with distinct burrows between 688 and 630 cm. The sediment between 630 and 467 cm is bioturbated, stratified mud with layering disturbed by bioturbation (Fig. 4c). The uppermost part of this unit has high sand content and marks the transition to the upper lithofacies unit.

The upper lithofacies from 467 to 0 cm, which represents deglaciation and the Holocene (Jennings et al., 2017), has overall lower CT number (lower density) (Fig. 3A), lower magnetic susceptibility (Fig. 3C) and generally lower sand content (Fig. 3D). But, it has much higher numbers of >2mm clasts (IRD) (Fig. 3B). Immediately above the boundary the sediments are low-density bioturbated mud with the sand fraction comprising *Coscinodiscus* planktic diatoms and setae of *Chaetoceras*, consistent with the low MS values (Fig. 3c). Well-defined, thin laminae and rare IRD occur at the base of the

unit, but transition upward to less-well defined laminae and rare to absent IRD from 420 cm to 352 cm. This fine interval was interpreted to record a period in the initial deglaciation as the grounding line retreated off the shelf edge with retention of an ice shelf (Jennings et al., 2017). At 352 cm (marked by middle horizontal blue line on Figure 3) the CT # (density), MS and sand increase (Fig. 3A, B, C, D). This level marks the start of renewed retreat of the GIS grounding line by calving (Jennings et al., 2017). The sediments are bioturbated but stratification is still evident, suggesting moderate sedimentation rates. Apart from a peak in >2mm clasts of west Greenland provenance at 330 cm the main rise in >2mm clasts coincides with the entry of the Northern Baffin Bay sediment source (NBB source) at 290 cm (Fig. 3B, E). Bioturbated, pebbly mud associated with a rise in NBB provenance occurs between 280 and 175 cm with the highest IRD interval from 280-240 cm (Fig. 3B, E). This NBB DC interval has been found in several cores on the central West Greenland slope (Sheldon et al., 2016; Jennings et al., 2017; Jackson et al., 2017) and has been correlated to BBDC1 (Simon et al., 2012; 2014; Jackson et al., 2017), marking the retreat of NBB ice streams. The NBB DC event is overlain by bioturbated mud with small, dispersed IRD and discontinuous silt stringers between 175 and 152 cm. Bioturbated pebbly mud between 152 and 52 cm has high NBB provenance between 160 and 90 cm, an interval that contains an age reversal and a mixture of radiocarbon ages (Fig. 3F). The age reversal suggests that the upper NBB peak is reworked. The upper 52 cm of the core is bioturbated mud with dispersed IRD likely represents the middle to late Holocene time period, although it is undated.

4.2 Biological Proxies

Biological proxy data are expressed against age using the age model based on ΔR=140 yrs (Fig. 5).

4.2.1 Bioturbation

The CT scan image (Fig. 3) reveals that the entire core is bioturbated, indicating that there was sufficient oxygenation and food to support the benthos in Baffin Bay throughout the time period represented by the core (Löwemark et al., 2012). Variations in burrow shape and density are indicative of the interplay between oxygenation, sedimentation rate, sedimentation processes, substrate consistency and food supply (Reineck and Singh, 1980, Wetzel, 1991; Löwenmark et al., 2012) (Fig. 4). Intensely bioturbated intervals in which sand layers are disrupted by burrowing (e.g. Fig. 4a, c, e) suggest periods of relatively slow sedimentation (Wetzel, 1991), whereas intervals of vertical burrows terminated by overlying strata (e.g. Fig. 4d, f) indicate episodic rapid sedimentation (Jennings et al., 2011a). Figure 4 shows expanded views of segments of the CT image shown in full on Figure 3 to illustrate some of the key lithofacies characteristics and trace fossil types that provide evidence for sedimentation processes. Muddy intervals typically have vertical burrows that are truncated by subsequent strata (Fig. 4d). These mud intervals likely represent plumites deposited from turbid meltwater plumes, whereas the sandy, stratified intervals with varying degrees of bioturbation likely represent distal turbidites (Ó Cofaigh and Dowdeswell, 2001) (Fig. 4c, f).

4.2.2 Foraminifera and Stable Isotopes

The Foraminiferal abundances in 12PC are spiky, with intervals of low benthic and planktic numbers per gram of dry sediment punctuated by periods of much higher numbers of foraminifers per gram (Fig. 5D). The high variability in abundance relates to

354 variations in marine productivity, overprinted by carbonate dissolution, and dilution by
355 high (12.8 cm/ka on average from 250-860 cm) and varying sedimentation rates. The
356 lithofacies characteristics suggest widely varying sedimentation rates in the core that are
357 not captured by the less frequent age control. Therefore we did not attempt to calculate
358 foraminiferal flux, which would have been a more direct measure of productivity, but
359 rather rely on foraminiferal numbers per gram as a measure of productivity.
360 *N. pachyderma*, the only planktic species, forms abundance spikes up to 1620
361 specimens/g, with intervening periods of very low abundance to absence (Fig. 5). The
362 planktic forams were quite small from the base of the core to 860 cm (22 cal ka BP), but
363 increased in size above that level. In general the planktic and benthic foram abundances
364 rise and fall together, suggesting that the abundance spikes represent *in situ* productivity
365 and a link between surface productivity and benthic food supply, although we cannot
366 control for variations in carbonate preservation. Low numbers of *N. pachyderma* per
367 gram are consistent with low productivity under perennial sea ice and the high numbers
368 per gram are consistent with periods of more open water, such as leads or polynyas in
369 summer (e.g. Nørgaard-Pedersen et al., 2003). Advection of planktic foraminifers from
370 outside Baffin Bay is unlikely, especially given the linkage between the benthic and
371 planktic productivity (cf Knutz et al., 2011; Nørgaard-Pedersen et al., 2003).
372 Oxygen isotope values on *N. pachyderma* ranged between 5.4 and 2 ‰. The
373 interval between 22 and 18.2 cal ka BP has mostly heavy values that fall between 4 and 5
374 ‰ (Fig. 5), comparable to MIS 2 values in the Fram Strait (Nørgaard-Pedersen et al.,
375 2003). A shift to lighter $\delta^{18}O$ and $\delta^{13}C$ values begins at 18 cal ka BP, suggests reduced
376 ventilation (Sarnthein et al., 1995). This interval falls within HS1 regardless of which ΔR

is applied (Fig. 2; Table 1). Above this shift the $\delta^{18}O$ values remain above 3.7 ‰. A pronounced light $\delta^{18}O$ spike at 19.4 cal ka BP corresponds to high planktic abundance and increased IP_{25} and Brassicasterol (Fig. 5). Oxygen isotopic values of this magnitude can either be related to glacial meltwater, especially if they are paired with light $\delta^{13}C$ values (Sarnthein et al., 1995) or to increased rate of sea-ice production that can produce brines with a light isotopic signature (Hillaire-Marcel et al., 2004; Hillaire-Marcel and de Vernal, 2008). The overall trend in the $\delta^{13}C$ values is toward heavier values suggesting better ventilation at the top of the record than at the bottom (Fig. 5).

The benthic foraminiferal assemblages (Fig. 6) provide insights into the productivity of surface waters, stratification of the water column, and turbid glacial meltwater influx. For example, sea-ice edge migration, either seasonal or in the form of leads or polynyas, produces pulses of phytoplankton production that sink to the seabed, providing food for benthic communities. The three most common benthic foraminiferal species in 12PC are *Stainforthia feylingi*, *Cassidulina reniforme* and *Elphidium excavatum* forma *clavata*. *S. feylingi* is dominant in conditions of stratified water column with a cold freshwater lid and has been associated with productivity at the seasonal sea ice edge (Seidenkrantz, 2013). It has been found in high abundances associated with biosiliceous sediments (Jennings et al., 2006). *E. excavatum* and *C. reniforme* occur together in glacial marine settings (Hald and Korsun, 1997). *C. reniforme* is also considered to represent chilled Atlantic Water (Slubowska et al., 2005) and is found in areas of relatively high, stable salinities (Polyak et al., 2002). *E. excavatum* is an opportunistic species that thrives in unstable environmental conditions influenced by rapid sedimentation and fluctuating salinities from turbid meltwater plumes (Hald and

Korsun, 1997). The agglutinated species, *Spiroplectammina biformis*, which occurs mainly in the lower lithofacies unit is found in arctic fjords with strong meltwater signal (Jennings and Helgadottir, 1994; Schaffer and Cole, 1986).

Several species indicative of marine productivity associated with nutrient rich Atlantic Water occur in both the lower and upper lithofacies unit: *Melonis barleeanus, Buccella frigida, Nonionella turgida* and *Nonionellina labradorica*. *Islandiella norcrossi* and *I. helenae* both are arctic species, but *I. helenae* is associated with sea-ice edge productivity while *I. norcrossi* reflects chilled Atlantic Water of normal marine salinity (Polyak et al., 2002; Wollenburg et al., 2004; Lloyd, 2006). *I. norcrossi* is a common calcareous species on the west Greenland shelf associated with Atlantic Water in the West Greenland Current (e.g. Lloyd, 2006; Perner et al., 2012).

Near the top of the lower unit (16.5 cal ka BP), and continuing into the base of the overlying biosiliceous mud, several species associated with marine productivity and nutrient rich Atlantic Water spike to high percentages. These include *N. turgida*, *M. barleeanus*, *B. frigida*, *I. norcrossi* and very low percentage of *Pullenia bulloides*. Current indicator species, *Cibicides lobatulus* also increases at this boundary. The central part of the diatom-rich mud is barren of calcareous foraminifers and is characterized by low faunal abundances dominated by agglutinated foraminiferal species (e.g. *Textularia earlandi*), suggesting that dissolution of carbonate likely overprinted the assemblages. The upper part of the diatom-rich mud shows a return of several of the marine productivity species along with increased percentages of *P. bulloides*, a chilled Atlantic water species, that is common on the SE Greenland and Northern Iceland shelves under

422 conditions of strong Irminger Current Atlantic water inflow (Eiríksson et al., 2000;
423 Jennings et al., 2011b).

424 Above the diatom-rich mud, the percentages of *N. labradorica* and *I. norcrossi*
425 increase, and *S. feylingi* continues with high percentages. The chilled Atlantic Water
426 species, *Cassidulina neoteretis*, is abundant at the top of the dated section along with *I.*
427 *norcrossi*, consistent with intermediate Atlantic Water and less prominent glacial
428 meltwater influence (Jennings and Helgadottir, 1993). The gap in foraminifers between
429 12 and 13.9 cal ka BP is likely a consequence of carbonate dissolution as other cores
430 from the central West Greenland margin, but in slightly shallower water (JR175-VC29;
431 Fig. 1) have *C. neoteretis* continuously between 14 and 11 cal ka BP (Jennings et al.,
432 2017).

433 *4.2.3 Biomarkers*

434 Further evidence of marine productivity and sea ice comes from the algal biomarkers
435 brassicasterol and IP_{25} (Fig. 5). In general, the presence of IP_{25} indicates release from
436 melting seasonal sea ice (Fahl and Stein, 2012; Belt et al., 2013), while the absence of
437 IP_{25} is consistent with intervals of thick perennial sea ice cover or no ice cover at all (Fahl
438 and Stein, 2012). Brassicasterol implies productivity in open-water conditions, but it also
439 can come from melting sea ice (Belt et al., 2013). In addition, the occurrence of polynyas
440 has been given as a possible reason for presence of IP_{25} and brassicasterol under
441 otherwise heavy ice conditions, even in the central Arctic Ocean (Xiao et al., 2013).

442 In the lower, high CT lithofacies unit of 12PC, brassicasterol and IP_{25} are present
443 in low abundances from 26 to 22 ka (ΔR=140 yrs), coinciding with low foraminiferal
444 abundances (Fig. 5). Between 22 and 20 ka, brassicasterol rises but IP_{25} is low to absent.

Foraminiferal abundances rise in this interval and the benthic fauna is characterized by productivity species (*B. frigida*, *I. helenae*, *M. barleeanus* and *N. labradorica*). An overall rise in IP_{25} and a large peak in brassicasterol occur at 19.5 ka, and continue with moderate values until another rise in brassicasterol values within the diatom-rich mud unit (16.2 to 15.1 cal ka BP). Both IP_{25} and brassicasterol continue to rise after 15.1 cal ka BP, but IP_{25} in particular rises to values unprecedented in the core after 14.3 cal ka BP.

This pattern of presence of IP_{25} and brassicasterol in the lower lithofacies unit argues for seasonal sea ice and some open water, although the generally low concentrations suggest that these were both likely less than in the upper unit - probably due to more extensive ice cover and only periodic opening - possibly as leads or polynyas. As the final increase in IP_{25} beginning at 16.2 ka is accompanied by rising, high brassicasterol it likely points to development of a marginal ice zone where there is increased marine productivity with probably more seasonal sea ice presence than before.

5. Discussion

5.1 Did an LGM Ice Shelf cover Baffin Bay?

There has been limited research on the LGM within Baffin Bay, which explains how the Baffin Bay ice shelf concept has remained untested. Radiocarbon dates on planktic foraminifers indicate that other cores besides 12PC have planktic fauna in the LGM. Andrews et al (1998) obtained a pair of AMS ^{14}C dates from abundant planktic foraminifera in southern Baffin Bay core HU77029-017PC (17,990 ± 110, and 17,930 ± 210 ^{14}C yrs; Andrews et al., 1998) (Fig. 1). These ^{14}C ages calibrate to the LGM (~21 ka BP; ΔR=140 years). A ^{14}C date on planktic foraminifers from core HE006-4-2PC

(21,440± 140 ^{14}C yrs) on the northern side of the Uummannaq TMF (Fig. 1) calibrates to ~25 ka BP (ΔR=140 years) (Ó Cofaigh et al., 2013a). In the LGM interval of 12PC (1130 cm to at least 690 cm) when the modeled Baffin Bay ice shelf would be in place, there are multiple lines of evidence for biological activity, including bioturbation, algal biomarkers and benthic and planktic foraminifers (Figs. 3 - 6). These findings are consistent with perennial sea-ice cover with some open water in the form of leads or polynyas on the eastern side of Baffin Bay. Full ice-shelf cover from an ice shelf extending from the Hudson Strait ice stream and grounding on Davis Strait all the way to Greenland (Alvarez-Solas et al., 2010; 2011; Marcott et al., 2011) would not allow the surface productivity (e.g. algal biomarkers, planktic forams) in Baffin Bay that would be needed to feed the benthic organisms that are evident (bioturbation and benthic foraminifers). On this basis we reject the modeling result of a full Baffin Bay ice shelf. While life has been observed under modern ice shelves in Antarctica, it is dependent on strong ocean inflow to the sub ice-shelf cavity from outside the ice shelf (Post et al., 2014). In the case of the Baffin Bay ice shelf cover as it is modeled, it would be sealed from the Labrador Sea marine advection and food supply.

The idea of the Davis Strait grounded ice shelf sprang in part from efforts to test a mechanism for Heinrich Event 1 (H1), in which subsurface warming reconstructed in the N. Atlantic in response to reduced Atlantic meridional overturning circulation (AMOC) during HS1 (McManus et al., 2004) weakens a buttressing ice shelf fronting the Hudson Strait ice stream and produces a Heinrich event (Álvarez-Solas et al., 2010; 2011; Marcott et al., 2011). Hulbe et al. (2004) modified their original 1997 Labrador Sea ice shelf idea to support instead fringing ice shelves along the coasts in Eastern Canada that

were proposed to have met their demise through a process of meltwater infilling of surface crevasses. The existence of this type of ice shelf and H-event process has been contested (Alley et al., 2005), but it is more consistent with the 12PC data than the original idea of an ice shelf grounding on Davis Strait (Hulbe et al., 1997).

5.2 Heinrich Stadial Environments

The data in 12PC allow examination of the environmental response in Baffin Bay to the transition from LGM to HS1, and the response in Baffin Bay to the large ice discharge from Hudson Strait during H1 which occurred when subsurface ocean heat was at a maximum and AMOC at a minimum (Marcott et al., 2011). Locating the LGM/HS1 transition and H1 in 12PC is made difficult by the uncertainties in the magnitude of the local marine reservoir age through time (Fig. 3F) (Stern and Lisiecki, 2013). The accepted timing of H1 calving event is 16.8 ka BP (Hemming, 2004), although it may be closer to 16 ka BP based on the timing of the peak of IRD in the North Atlantic IRD stack during HS1 (Stern and Lisiecki, 2013). If we apply the ΔR envelope approach using data from Stern and Lisiecki (2013) to the mean value of the best 2 constraining radiocarbon ages from the base of DC1 (=H1) in cores HU75009-IV-055PC and HU87033-009 LCF (Fig. 1; Andrews et al., 1994; Jennings et al., 1996), from the Labrador Sea, we obtain a range of ages for the event that spans HS1 (Table 1). The ΔR that matches best the H1 16.8 ka age determined by Hemming (2004) is the lower ΔR from Stern and Lisiecki (2013) (Table 1). On this basis, we chose to use the Lower ΔR to determine where HS1 lies in the 12PC record. Lower ΔR places the base of HS1 (18 ka BP) at 610 cm and its end (14.7 ka BP) at 395cm, right at the end of the diatom-rich mud unit and before the initiation of calving retreat (Fig. 3F and 7). Lower ΔR also puts the

514 calving retreat and the timing of the west Greenland DC event (=BBDC1; Jackson et al.,
515 2017) (Fig. 3) in the Bølling/Allerød interstadial (Fig. 7). The age model calculated with
516 an invariant ΔR=140 years places the lithofacies transition which represents the
517 grounding line retreat from the west Greenland shelf edge at 16.2 cal ka BP, within HS1
518 (Jennings et al., 2017), but places the end of HS1 after the initiation of GIS calving
519 retreat.

520 Figure 7 illustrates how key proxy data map into the Heinrich Stadial interval
521 defined by evidence of sluggish AMOC (McManus et al., 2004) using the lower ΔR of
522 Stern and Lisiecki (2013). In the Labrador Sea HS1 is an interval of anomalously warm
523 bottom waters (Marcott et al., 2011) within which H1 occurred (Fig. 7). We would
524 expect this massive freshwater (meltwater and icebergs) outflow from collapse of the
525 Hudson Strait ice stream (Andrews and Tedesco, 1992; Hesse and Khodabakhsh, 2016)
526 to perturb environments in Baffin Bay or initiate a transition to different
527 paleoceanographic conditions.

528 The transition to lighter $\delta^{18}O$ values and a shift to very high percentages of *S.*
529 *feylingi* coincide with HS1 (Fig. 7). This signal is also seen in nearby core JR175-VC29
530 (Fig. 1), from 900 m water depth (Jennings et al., 2017) and is associated in both 12PC
531 and VC29 with deposition of diatom-rich mud with rare IRD; a fine-grained unit of
532 similar age is observed in core GeoTü SL-170 (Jackson et al., 2017) slightly north of
533 VC29. The diatom-rich mud interval has been interpreted by Jennings et al. (2017) to
534 indicate exclusion of coarse sediment delivery to the Disko TMF by retention of a
535 fringing ice shelf after initial grounding line retreat. Overall, brassicasterol abundances
536 are low in HS1. A period of high productivity of benthic forams indicative of nutrient

537 rich Atlantic water at the subsurface (Fig. 5) (indicated on Fig. 7 by red stars and low
538 percentages of the benthic foraminiferal species, *S. feylingi*) coincides with the initial
539 GIS retreat from the shelf edge as indicated in the CT# profile (Jennings et al., 2017).
540 Subsequent interstadial conditions are marked by rising marine productivity, renewed
541 subsurface Atlantic Water influence, and renewed retreat of the GIS, followed by
542 development of consistent seasonal sea ice and release/melting of detrital carbonate
543 bearing ice bergs from ice margins of northern Baffin Bay termed a west Greenland DC
544 event by (Jennings et al., 2017) that has been shown to be correlative to BBDC1 (Simon
545 et al. (2016) by Jackson et al. (2017).
546
547 **6. Conclusions**
548 1. Based on the data presented we reject the hypothesis that Baffin Bay was covered by a
549 full ice shelf during the LGM. We conclude instead that Baffin Bay was perennially sea-
550 ice covered with nutrient rich, relatively warm Atlantic water present at depth through the
551 LGM. Evidence of marine productivity suggests that there were openings in the sea-ice
552 cover as leads and polynyas to support marine productivity. Concurrently, sediment-
553 laden, glacial-meltwater and turbidity currents were released from the GIS, grounded at
554 the shelf edge, but IRD was rare suggesting the ice front was protected by a fringing ice
555 shelf and/or the perennial sea-ice cover.
556 2. Reduced ventilation and productivity, coincident with a cold surface lid of meltwater
557 was established in HS1. After Heinrich Event 1, but within the Heinrich stadial, an
558 interval of increased productivity and Atlantic Water is associated with the retreat of the
559 GIS grounding line from the shelf edge.

560 3. The implication for Heinrich Events and Ocean warming/Ice Shelf hypothesis is that
561 perennial sea-ice cover and/or fringing ice shelves may be sufficient to explain the heat
562 retention and back-pressure proposed to explain the dynamics that produce Heinrich
563 Events.
564
565 **7. Acknowledgements**
566 Funding for this research was provided by the US National Science Foundation grant
567 ARC1203492 and the UK Natural Environment Research Council grant NE/D001951/1.
568 We thank the captain, crew and scientists aboard the 2008 CSS Hudson cruise HU2008-
569 029 for acquisition of core 2009029-12PC. We gratefully acknowledge the microscope
570 and x-ray diffraction research by undergraduate research assistants, Brian Shreve,
571 Jennifer Kelly, Matthew Reed, and Matthew Glasset. We thank Quentin Simon and one
572 anonymous reviewer for helpful critique of the manuscript.
573
574 **8. Figure Captions**
575 Figure 1. Bathymetric map centered on Baffin Bay (BB) showing the location of core
576 HU2008029-12PC (12PC) and other cores mentioned in the text, the distribution of
577 Paleozoic carbonate bedrock, mapped ice margin positions in northern Baffin Bay (Li et
578 al., 2011) and central west Greenland (Ó Cofaigh et al., 2013a) and major ice streams.
579 UIS = Uummannaq ice stream; DIS = Disko ice stream; SSIS = Smith Sound ice stream;
580 LSIS = Lancaster Sound ice stream. Northward flowing West Greenland Current (WGC)
581 is shown as the thin red line and the southward flowing Baffin Current (BC) is shown as
582 a thin blue line. The position of the acoustic profile in Figure 2 is shown as a black line.

583 HU2008029-016PC=16; HE006-4-2PC=2; JR175-VC29=29; HU77029-017PC=17;
584 HU75009-IV-055PC=55 and HU87033-009 LCF=9. Inset plot shows the salinity and
585 temperature against water depth at from the same location as 2008029-12PC.
586 ASW=Arctic Surface Water; WGIW=West Greenland Intermediate Water; DBBW=Deep
587 Baffin Bay Water.
588
589 Figure 2. A. 3.5 kHz sub-bottom profile over the site of 2008029-12PC demonstrationg
590 the acoustically-stratified character of the seabed in the area. B. A zoom in map of the 3.5
591 kKz sub-bottom profile and the core location shown in Figure 1. The bathymetry is from
592 GEBCO.
593
594 Figure 3. Lithological proxies and age control for 2008029-12PC. A is the CT image
595 against depth in the core. Black bars along depth axis show the locations of CT images
596 shown in Figure 4. ‘V’ denotes locations of vertical burrows. B. IRD counts (>2mm
597 clasts) from CT scan in 2 cm increments. C. CT number, a measure of density derived
598 from the CT image. D. Magnetic Susceptibility measure by multi sensor track (MST). E.
599 Weight percentage of >63 μm sand fraction from foraminiferal samples. F. Two-source
600 provenance of minerals: Northern Baffin Bay (NBB, brown) vs. the local source, central
601 west Greenland (green). F. Depth-Age model in pink (ΔR=140±30 yrs) showing 1σ and
602 2 σ uncertainties of the model. Excluded from the model are benthic foraminiferal ages
603 (green distributions) and outliers at 1 meter. Age envelope for other potential ΔR
604 calibrations are shown by blue (ΔR=0); Red, green, orange = lower, mean, and upper ΔR
605 values from Stern and Lisiecki (2013). Climate units are along the age scale.

606

607 Figure 4. Examples of lithofacies and bioturbation types from 2008029-12PC CT scans.
608 See Figure 3 for locations of these examples on the CT image of the core.

609

610 Figure 5. Biological proxies from 12PC compared with CT# plot to assist with
611 comparison to depth on depth in Figure 3. A. CT#; B. sea ice biomarker, IP_{25}; C. marine
612 productivity biomarker, brassicasterol; D. Benthic (blue) and planktic (red) forams per
613 gram of dry sediment; E. $\delta^{18}O$ of planktic foraminifer, *N. pachyderma*, blue; F. $\delta^{13}C$ of *N.*
614 *pachyderma*, green.
615 Figure 6. Benthic foraminiferal species in 12PC. Green represent marine productivity
616 species; Red=Atlantic Water species; Blue = Arctic species; Light Blue; Glacial marine
617 species; Orange=transformed (cooler and slightly lower salinity) Atlantic Water species.

618

619 Figure 7. Comparison between Pa/Th record of AMOC (McManus et al., 2004) and the
620 timing of Heinrich Event 1 (H1) to key paleoenvironmental proxies in 12PC. The HS1
621 interval (yellow box) is defined in the core with use of the Lower ΔR of Stern and
622 Lisiecki (2013) (Fig. 3f). Blue lines show where key events in the core map into the
623 climatic intervals with use of the Lower ΔR of Stern and Lisiecki (2013). A. CT # from
624 12PC; B. Brassicasterol, 12PC; C. IP_{25}, 12PC; D. *Stainforthia feylingi*, 12PC; E. Oxygen
625 isotope ratios, 12PC; F. Pa/Th ratios (McManus et al., 2004).

626 **References Cited**
627
628 Aksu, A. E., 1985. Climatic and oceanographic changes over the past 400,000 years:
629 Evidence from deep-sea cores on Baffin Bay and David Strait. *In* Andrews, J. T. (ed.),
630 *Quaternary Environments: Eastern Canadian Arctic, Baffin Bay and Western*
631 *Greenland*. Boston: Allen and Unwin, 181-209.

Alley, R. B., Andrews, J. T., Barber, D. C., and Clark, P. U., 2005: Comment on "Catastrophic ice shelf breakup as the source of Heinrich event icebergs" by C.L. Hulbe et al. *Palaeoceanography,* 20: doi:10:1029/2004PA001086.

Álvarez-Solas, J., Charbit, S., Ritz, C., Paillard, D., Ramstein,G., and Dumas, C.: Links between ocean temperature and icebergdischarge during Heinrich events, *Nature Geoscience*, 3, 122–126, 2010

Álvarez-Solas, J., Montoya, M., Ritz, C., Ramstein, G., Charbit, S., Dumas, C., Nisancioglu, K., Dokken, T., Ganopolski, A., 2011. Heinrich event 1: an example of dynamical ice-sheet reaction to ocean changes. *Climate of the Past* 7, 1297-1306. doi:10.5194/cp-7-1297-2011.

Andrews, J.T., Eberl, D.D., 2011. Surface (sea floor) and near-surface (box cores) sediment mineralogy in Baffin Bay as a key to sediment provenance and ice sheet variations. *Can. J. Earth Sci.* 48 (9), 1307 - 1328. http://dx.doi.org/10.1139/-11-021.

Andrews, J.T., Eberl, D.D., 2012. Determination of sediment provenance by unmixing the mineralogy of source-area sediments: The "SedUnMix" program. *Marine Geology* 291, 24-33.

Andrews, J.T., Erlenkeuser, H., Tedesco, K., Aksu, A., Jull, A.J.T., 1994. Late Quaternary (Stage 2 and 3) Meltwater and Heinrich events, NW Labrador Sea. *Quaternary Research* 41, 26-34.

Andrews, J.T, Gibb, O.T., Jennings, A.E., Simon, Q., 2014. Variations in the provenance of sediment from ice sheets surrounding Baffin Bay during MIS 2 and 3 and export to the Labrador Shelf Sea: site HU2008029-0008 Davis Strait. *Journal of Quaternary Science* 29, 3-13.

Andrews, J. T., Kirby, M. E., Aksu, A., Barber, D. C., and Meese, D., 1998. Late Quaternary Detrital Carbonate (DC-) events in Baffin Bay (67° - 74° N): Do they correlate with and contribute to Heinrich Events in the North Atlantic? *Quaternary Science Reviews,* 17: 1125-1137.

Andrews, J. T. and Tedesco, K., 1992: Detrital carbonate-rich sediments, northwestern Labrador Sea: Implications for ice-sheet dynamics and iceberg rafting (Heinrich) events in the North Atlantic. *Geology,* 20: 1087-1090.

Belt, S.T., Brown, T.A., Navarro Rodriguez, A., Cabedo Sanz, P., Tonkin, A., Ingle, R., 2012. A reproducible method for the extraction, identification and quantification of the Arctic sea ice proxy IP25 from marine sediments. *Analytical Methods* 4, 705-713.

Belt, S.T., Brown, T.A., Ringrose, A.E., Cabedo-Sanz, P., Mundy, C.J., Gosselin, M., Poulin, M., 2013. Quantitative measurement of the sea ice diatom biomarker IP25

and sterols in Arctic sea ice and underlying sediments: Further considerations for palaeo sea ice reconstrucion. *Organic Geochemistry* 62, 33–45.

Belt, S.T., Cabedo-Sanz, P., Smik, L., Navarro-Rodriguez, A., Berben, S.M., Knies, J., Husum, K., 2015. Identification of paleo Arctic winter sea ice limits and the marginal ice zone: Optimised biomarker-based reconstructions of late Quaternary Arctic sea ice. *Earth and Planetary Science Letters* 431, 127-139.

Blake, W., Jr. 1977. Glacial sculpture along the east-central coast of Ellesmere Island, Arctic Archipelago. Current Research, Part C, Geological Survey of Canada, Paper 77-1C, 107-115.

Briner, J. P., Miller, G. H., Davis, P. T., Bierman, P. R., and Cafee, M., 2003. Last Glacial Maximum ice sheet dynamics in Arctic Canada inferred from young erratics perched on ancient tors. *Quaternary Science Reviews,* 22: 437-444.

Brown, T.A., Belt, S.T., 2012. Closely linked sea ice–pelagic coupling in the Amundsen Gulf revealed by the sea ice diatom biomarker IP25. Journal of plankton research 34, 647-654.

Buch E. 2000a. A monograph on the physical oceanography of the Greenland waters. Danish Meteorological Institute Scientific Report, 00-12.

Buch E. 2000b. Air-sea-ice conditions off southwest Greenland, 1981–1997. *Journal of Northwest Atlantic Fisheries Science* 26, 1–14.

Buizert, C., Gkinis, V., Severinghaus, J.P., He, F., Lecavalier, B.S., Kindler, P., Leuenberger, M., Carlson, A.E., Vinther, B., Masson-Delmotte, V., White, J.W.C., Liu, Z., Otto-Bliesner, B., Brook, E.J., 2014. Greenland temperature response to climate forcing during the last deglaciation. Science 345, 1177-1180. DOI: 10.1126/science.1254961

Campbell, D C, de Vernal, A., 2009. CCGS Hudson Expedition 2008029: marine geology and paleoceanography of Baffin Bay and adjacent areas, Nain, NL to Halifax, NS, August 28-September 23. Geological Survey of Canada, Open File 5989, 2009, 212 pages; 1 DVD, doi:10.4095/261330

Clark, P.U., Dyke, A.S., Shakun, D., Carlson, A.E., Clark, J., Wohlfarth, B., Mitrovica, J.X., Hostetler, S.W., McCabe, A.M., 2009. The Last Glacial Maximum. Science 325, 710-714.

Dahl-Jensen, D. and al., e., 1998: Past Temperatures Directly from the Greenland Ice Sheet. *Science,* 282: 268-271.

722 Darling, K. F., Kucera, M., Kroon, D., Wade, C.M., 2006. A resolution for the coiling
723 direction paradox in *Neogloboquadrina pachyderma*. *Paleoceanography* 21,
724 PA2011, doi:10.1029/2005PA001189.
725
726 de Vernal, A., Bilodeau, G., Hillair -Marcel, C., Kassou, N., 1992. Quantitative
727 assessment of carbonate dissolution in marine sediments from foraminifer linings
728 vs. shell ratios: example from Davis Strait, NW North Atlantic, Geology, 20: 527-530.
729
730 Domack, E.W., Harris, P.T., 1998. A new depositional model for ice shelves, based
731 upon sediment cores from the Ross Sea and the Mac. Roberson shelf, Antarctica.
732 *Annals of Glaciology* 27, 281-284.
733
734 Dowdeswell, J.A., Hogan, K.A., Ó Cofaigh, C., Fugelli, E.M.G., Evans, J., Noormets, R.,
735 2014. Late Quaternary ice flow in aWest Greenland fjord and cross-shelf trough
736 system: submarine landforms from Rink Isbrae to Uummannaq shelf and slope.
737 *Quat. Sci. Rev.* 92, 292-309. http://dx.doi.org/10.1016/j.quascirev.2013.09.007.
738
739 Dyke, A. S., Andrews, J. T., Clark, P. U., England, J. H., Miller, G. H., Shaw, J., and
740 Veillette, J. J., 2002: The Laurentide and Innuitian ice sheets during the Last Glacial
741 Maximum. *Quaternary Science Reviews,* 21, 9-31.
742
743 Eberl, D.D., 2003. User guide to RockJock: A program for determining quantitative
744 mineralogy from X-ray diffraction data. United States Geological Survey, Open File
745 Report 03-78, 40 pp, Washington, DC.
746
747 Eiríksson, J., Knudsen, K.L., Haflidason, H., Henriksen, P., 2000. Late-glacial and
748 Holocene palaeoceanography of the North Icelandic shelf. J*ournal of Quaternary*
749 *Science* 15, 23-42.
750
751 England, J. 1999. Coalescent Greenland and Innuitian ice during the Last Glacial
752 Maximum: Revising the Quaternary of the Canadian High Arctic. *Quaternary Science*
753 *Reviews* 18, 421–426, http://dx.doi.org/10.1016/S0277-3791(98)00070-5.
754
755 England, J., Atkinson, N., Bednarski, J., Dyke, A.S., Hodgson, D.A., Ó Cofaigh, C. 2006.
756 The Innuitian Ice Sheet: configuration, dynamics and chronology. *Quaternary*
757 *Science Reviews* 25, 689-703.
758
759 Fahl, K., Stein, R., 2012. Modern seasonal variability and deglacial/Holocene change
760 of central Arctic Ocean sea ice cover: New insights from biomarker proxy records.
761 *Earth and Planetary Science Letters* 351–352, 123–133.
762
763 Grobe, H., 1987. A simple method for the determination of ice-rafted debris in
764 sediment cores. *Polarforschung* 57 (3), 123-126.
765
766 Hald, M., Korsun, S. 1997. Distribution of modern benthic foraminifera from fjords of
767 Svalbard, European Arctic. *Journal of Foraminiferal Research* 27, 101–122.

Hemming, S.R., 2004. Heinrich events: massive late Pleistocene detritus layers of the North Atlantic and their global climate imprint. *Rev. Geophys.* 42, RG1005.

Hesse, R., Khodabakhsh, S. 2016. Anatomy of Labrador Sea Heinrich layers. *Marine Geology* 380, 44-86. http://dx.doi.org/10.1016/j.margeo.2016.05.019

Hesse, R., Khodabakhsh, S., Klaucke, I., Ryan, WBF., 1997. Asymmetrical turbid surface-plume deposition near ice-outlets of the Pleistocene Laurentide ice sheet in the Labrador Sea. *Geo-Marine Letters*, 17, 179-187.

Hillaire-Marcel, C., de Vernal, A., 2008. Stable isotope clue to episodic sea-ice formation in the glacial North Atlantic. Earth and Planetary Science Letters, 268, 143-150.

Hillaire-Marcel, C., de Vernal, A., Aksu, A.E., Macko, S., 1989. High-resolution isotopicand micropaleontological studies of upper Pleistocene sediments at ODP Site 645, Baffin Bay, Proceedings of the Ocean Drilling Program, 105B: 599-616.

Hofmann, J.C., Knutz, P.C., Nielsen, T., Kuijpers, A., 2016. Seismic architecture and evolution of the Disko Bay trough-mouth fan, central West Greenland margin, *Quaternary Science Reviews*, http://dx.doi.org/10.1016/j.quascirev.2016.05.019

Holland, D.M., Thomas, R.H., de Young, B., Ribergaard, M.H., Lyberth, B., 2008. Acceleration of Jakobshavn Isbræ triggered by warm subsurface oceanwaters. *Nature Geoscience* 1 (10), 659**e**664. http://dx.doi.org/10.1038/ngeo316.

Hulbe, C.L., 1997. An ice shelf mechanism for Heinrich layer production, *Paleoceanography* 12, 711 –717.

Hulbe, C. L., MacAyeal, D. R., Denton, G. H., Kleman, J., and Lowell, T. V., 2004: Catastrophic ice shelf breakup as the source for Heinrich event icebergs. *Palaeoceanography,* 19: 1 of 15, doi.10.1029/2003:PA000890, 002004.

Jackson, R., Carlson, A.E., Hillaire-Marcel, C., Wacker, L., Vogt, C., Kucera, M., 2017. Asynchronous instability of the North American-Arctic and Greenland ice sheets during the last deglaciation. *Quaternary Science Reviews* 164, 140-153. http://dx.doi.org/10.1016/j.quascirev.2017.03.020.

Jennings, A.E., Andrews, J.T., Ó Cofaigh, C., St. Onge, G., Sheldon, C., Belt, S.T., Cabedo-Sanz, P., Hillaire-Marcel, C. 2017. Ocean forcing of Ice Sheet Retreat in Central West Greenland from LGM through Deglaciation. *Earth and Planetary Science Letters* 472, 1-13 .

Jennings, A.E., Andrews, J.T., Wilson, L., 2011b. Holocene Environmental Evolution of the SE Greenland Shelf North and South of the Denmark Strait: Irminger and East Greenland Current Interactions. Quaternary Science Reviews 30: 980-998.

Jennings, A.E., Hald, M., Smith, L.M., and Andrews, J.T., 2006. Freshwater forcing from the Greenland Ice Sheet during the Younger Dryas: Evidence from southeastern Greenland shelf cores: *Quaternary Science Reviews* 25, 282–298, doi:10.1016/j.quascirev.2005.04.006.

Jennings, A.E., Helgadottir, G., 1994. Foraminiferal assemblages from the fjords and shelf of eastern Greenland. *J. Foraminifer. Res*. 24 (2), 123**e**144. http://dx.doi.org/10.2113/gsjfr.24.2.123.

Jennings, A.E., Sheldon, C., Cronin, T.M., Francus, F., Stoner, J, Andrews, J., 2011a. The Holocene history of Nares Strait, transition from glacial bay to Arctic-Atlantic throughflow. *Oceanography* 24, no. 3, 26-41.

Jennings, A. E., Tedesco, K. A., Andrews, J. T., and Kirby, M. E., 1996. Shelf erosion and glacial ice proximity in the Labrador Sea during and after Heinrich events (H-3 or 4 to H-0) as shown by foraminifera. *In* Andrews, J. T., Austin, W. E. N., Bergsten, H., and Jennings, A. E. (eds.), *Late Quaternary Palaeoceanography of the North Atlantic Margins*: Geological Society Special Publications, 29-49.

Jennings, A.E., Walton, M.E., Cofaigh, C._O., Kilfeather, A., Andrews, J.T., Ortiz, J.D., et al., 2014. Paleoenvironments during Younger Dryas-early Holocene retreat of the Greenland ice sheet from outer Disko Trough, central west Greenland. *J. Quat. Sci*. 29 (1), 27**e**40. http://dx.doi.org/10.1002/jqs.2652.

Kaufman, D.S., Williams, K.M. (compilers), 1992. Radiocarbon Date List VII: Baffin Island, N.W.T., Canada. INSTAAR Occasional Paper 48. Institute of Arctic and Alpine Research, University of Colorado, Boulder.

Knutz, P. C., M.-A. Sicre, H. Ebbesen, S. Christiansen, and A. Kuijpers, 2011. Multiple-stage deglacial retreat of the southern Greenland Ice Sheet linked with Irminger Current warm water transport, *Paleoceanography* 26, PA3204, doi:10.1029/2010PA002053.

Li, G., Piper, D. J. W., and Campbell, D. C., 2011: The Quaternary Lancaster Sound trough-mouth fan, NW Baffin Bay. *Journal of Quaternary Science,* 26: 511-522.
Lloyd, J. M. 2006. Modern distribution of benthic foraminifera from Disko Bugt, West Greenland. *Journal of Foraminiferal Research* 36, 315–331.

Lloyd, J.M., Moros, M., Perner, K., Telford, R.J., Kuijpers, A., Jansen, E., et al., 2011.A 100 yr record of ocean temperature control on the stability of JakobshavnIsbrae, West Greenland. *Geology* 39 (9), 867-870. http://dx.doi.org/10.1130/G32076.1.

Löwemark, L., O'Regan, M., Hanebuth, T.J.J., Jakobsson, M., 2012. Late Quaternary spatial and temporal variability in Arctic deep-sea bioturbation and its relation to Mn cycles. *Palaeogeography, Palaeoclimatology, Palaeoecology* 365-366, 192-208.

Lucci, RG and Rebesco, M., 2007. Glacial contourites on the Antarctic Peninsula margin: insight for palaeoenvironmental and palaeoclimatic conditions. Geological Society, London, Special Publications, 276: 111-127.

Marcott et al., 2011. Ice-shelf collapse from subsurface warming as a trigger for Heinrich Events. PNAS 108. No. 33 p. 13415-13419

McManus, J.F., Francois, R., Gherardi, J.-M., Keigwin, L.D., Brown-Leger, S., 2004. Collapse and rapid resumption of the Atlantic meridional circulation linked to deglacial climate change. Nature 428, 834-837.

Münchow A., Falkner, A. Melling, H., 2015. Baffin Island and West Greenland Current Systems in northern Baffin Bay. *Progress in Oceanography* 132, 305–317

Ó Cofaigh C., Andrews JT, Jennings AE, Dowdeswell JA, Hogan KA, Kilfeather AA, et al. (2013a) Glacimarine lithofacies, provenance and depositional processes on a West Greenland trough-mouth fan. *Journal of Quaternary Science* 28. Available at: http://dx.doi.org/10.1002/jqs.2569: doi:10.1002/jqs.2569.

Ó Cofaigh C, Dowdeswell J.A., 2001. Laminated sediments in glacimarine environments: diagnostic criteria for their interpretation. *Quaternary Science Reviews* 20, 1411-1436.

Ó Cofaigh C., Dowdeswell J.A., Jennings A.E., Hogan K.A., Kilfeather A., Hiemstra J.F., et al. (2013b) An extensive and dynamic ice sheet on the West Greenland shelf during the last glacial cycle. *Geology* 41(2): 219–222: doi:10.1130/G33759.1.

Nørgaard-Pedersen, N., Spielhagen, R.F., Erlenkeuser, H., Grootes, P.M., Heinemeier, J., Knies, J. , 2003. Arctic Ocean during the Last Glacial Maximum: Atlantic and polar domains of surface water mass distribution and ice cover. Paleoceanography 18, doi:10.1029/2002PA000781, 2003.

Perner, K., Moros, M., Jennings, A., Lloyd, J.M., Knudsen, K.L., 2012. Holocene palaeoceanographic evolution off West Greenland. *The Holocene* 23, 374-387.

Piénkowski, A.J., England, J.H., Furze, M.F.A., Marret, F., Eynaud, F., Vilks, G., Maclean, B., Blasco, S., Scourse, J.D., 2012. The deglacial to postglacial marine environments of SEBarrow Strait, Canadian Arctic Archipelago. *Boreas* 41 (2), 141-179. http://dx.doi.org/10.1111/j.1502-3885.2011.00227.x.

Polyak, L., Korsun, S., Febo, L.A., Stanovoy, V., Khusid, T., Hald, M., Paulsen, B.E., Lubinski, D.J., 2002. Benthic foraminiferal assemblages from the southern Kara Sea,

a river influenced Arctic marine environment. *Journal Foraminiferal Research* 32, 252–273.

Post, A.L., Galton-Fenzi, B.K., Riddle, M.J., Herraiz-Borreguero, L., O'Brien, P.E., Hemer, M.A., McMinn, A., Rasch, D., Craven, M., 2014. Modern sedimentation, circulation and life beneath the Amery Ice Shelf, East Antarctica. *Continental Shelf Research* 74. 77-87.

Quillmann, U., Andrews, J. T., and Jennings, A. E., 2009: *Radiocarbon Date List XI: East Greenland shelf, West Greenland Shelf, Labrador Sea. Baffin Island shelf, Baffin Bay, Nares Strait, and Southwest to Northwest Icelandic shelf.* Occasional Paper No. 59, INSTAAR, University of Colorado, Boulder, Boulder.

Ramsey, C.B. and Lee, S., 2013. Recent and planned developments of the program OxCal. Radiocarbon 55, 720-730.

Reeh, N., Thomsen, H. H., Higgins, A. K., and Weidick, A., 2001: Sea ice and the stability of north and northeast Greenland floating glaciers. *In* Jeffries, M. O. and Eicken, H. (eds.), *Annals of Glaciology, Vol 33*, 474-480.

Reimer, P.J., Bard, E., Bayliss, A., Beck, J.W., Blackwell, P.G., Ramsey, C.B., Grootes, P.M., Guilderson, T.P., Haflidason, H., Hajdas, I., Hatté, C., Heaton, T.J., Hoffmann, D.L., Hogg, A.G., Hughen, K.A., Kaiser, K.F., Kromer, B., Manning, S.W., Niu, M., Reimer, R.W., Richards, D.A., Scott, E.M., Southon, J.R., Staff, R.A., Turney, C.S.M., van der Plicht, J., 2013. IntCal13 and Marine13 radiocarbon age calibration curves 0-50,000 years cal BP. Radiocarbon 55, 1869–1887. http://dx.doi.org/10.2458/azu_js_rc.55.16947.

Reineck, H.E., Singh, I.B., 1980. Depositional Sedimentary Environments. Springer-Verlag, NY.

Sarnthein, M., et al., Variations in Atlantic surface ocean paleoceanography, 50_–80_N: A time-slice record of the last 30,000 years, Paleoceanography, 10(6), 1063– 1094, 1995.
Schafer, C.T., Cole, F.E., 1988. Environmental associations of Baffin Island fjord agglutinated foraminifera. *Abh. Geol. Bundesanst*, 307.

Seidenkrantz, M.-S., 2013. Benthic foraminifera as palaeo sea-ice indicators in the subarctic realm-examples from the Labrador Sea-Baffin Bay region. *Quaternary Science Reviews* 79, 135-144. http://dx.doi.org/10.1016/j.quascirev.2013.03.014

Shaffer, G., Olsen, S.M., Bjerrum, C.J., 2004. Ocean subsurface warming as a mechanism for coupling Dansgaard-Oeschger climate cycles and ice-rafting events. Geophysical Research Letters 31, L24202. doi:10.1029/2004GL020968.

Sheldon, C., Jennings, A., Andrews, J.T., Ó Cofaigh, C., Hogan, K., Dowdeswell, J.A., Seidenkrantz, M-S., 2016. Ice stream retreat following the LGM and onset of the west

Greenland current in Uummannaq Trough, west Greenland. *Quaternary Science Reviews*, http://dx.doi.org/10.1016/j.quascirev.2016.01.019

Simon, Q., Hillaire-Marcel, C., St-Onge, G., Andrews, J.T., 2014. Northeastern Laurentide, western Greenland and southern Innuitian ice stream dynamics during the last glacial cycle. *Journal of Quaternary Science* 29(1): 14-26. DOI: 10.1002/jqs.2648

Simon Q, St-Onge G, Hillaire-Marcel C., 2012. Late Quaternary chronostratigraphic framework of deep Baffin Bay glaciomarine sediments from high-resolution paleomagnetic data. Geochemistry, Geophysics, Geosystems 13: Q0AO03. doi: 10.1029/ 2012GC004272

Simon, Q., Thouveny, N., Bourles, D.L., Nuttin, L., Hillaire-Marcel, C., St-Onge, G., 2016. Authigenic $^{10}Be/^{9}Be$ ratios and ^{10}Be-fluxes ($^{230}Th_{xs}$-normalized) in central Baffin Bay sediments during the last glacial cycle: Paleoenvironmental implications. *Quaternary Science Reviews* 140, 142-162.

Slabon, P., Dorschel, B., Jokat, W., Myklebust, R., Hebbeln, D., Gebhardt, C., 2016. Greenland ice sheet retreat history in the northeast Baffin Bay based on high-resolution bathymetry. *Quaternary Science Reviews* 154, 182-198. http://dx.doi.org/10.1016/j.quascirev.2016.10.022

Slubowska, M.A., Koç, N., Rasmussen, T.L., Klitgaard-Kristensen, D., 2005. Changes in the flow of Atlantic water into the Arctic Ocean since the last deglaciation: evidence from the northern Svalbard continental margin, 80_N. *Paleoceanography* 20, PA4014. doi:10.1029/2005PA001141.

Stern, J.V., Lisiecki, L.E. 2013. North Atlantic circulation and reservoir age changes over the past 41,000 years. Geophysical Research Letters 40: 3693-3697. doi:10.1002/grl.50679, 2013.

Straneo, F., Sutherland, D.A., Holland, D., Gladish, C., Hamilton, G.S., Johnson, H.L., Rignot, E., Xu, Y., Koppes, M., 2012. Characteristics of ocean waters reaching Greenland's glaciers. *Annals of Glaciology* 53(60), 202-210. doi:10.3189/2012AoG60A059

Tang, C.C.L., Ross, C.K., Yao, T., Petrie, B., DeTracey, B.M., Dunlap, E., 2004. The circulation, water masses and sea-ice of Baffin Bay. *Progress in Oceanography* 63, 183–228.

Wetzel, A., 1991. Ecologic interpretation of deep-sea trace fossil co=unities. Palaeogeography, Palaeoclimatology, Palaeoecology 85, 47-69.

Wollenburg, J.E., Knies, J., Mackensen, A., 2004. High-resolution paleoproductivity fluctuations during the past 24 kyr as indicated by benthic foraminifera in the

994 marginal Arctic Ocean. *Palaeogeography, Palaeoclimatology, Palaeoecology* 204, 209-
995 238.
996
997 Xiao, X., Fahl, K., Stein, R., 2013. Biomarker distributions in surface sediments from the
998 Kara and Laptev seas (Arctic Ocean): indicators for organic-carbon sources and sea ice
999 coverage. *Quaternary Science Reviews* 79, 40–52.
1000
1001 Zreda, M., J. England, F. Phillips, D. Elmore, and P. Sharma. 1999. Unblocking of the
1002 Nares Strait by Greenland and Ellesmere Ice-Sheet retreat 10,000 years ago. *Nature*
1003 398,139–142, http://dx.doi.org/10.1038/18197
1004

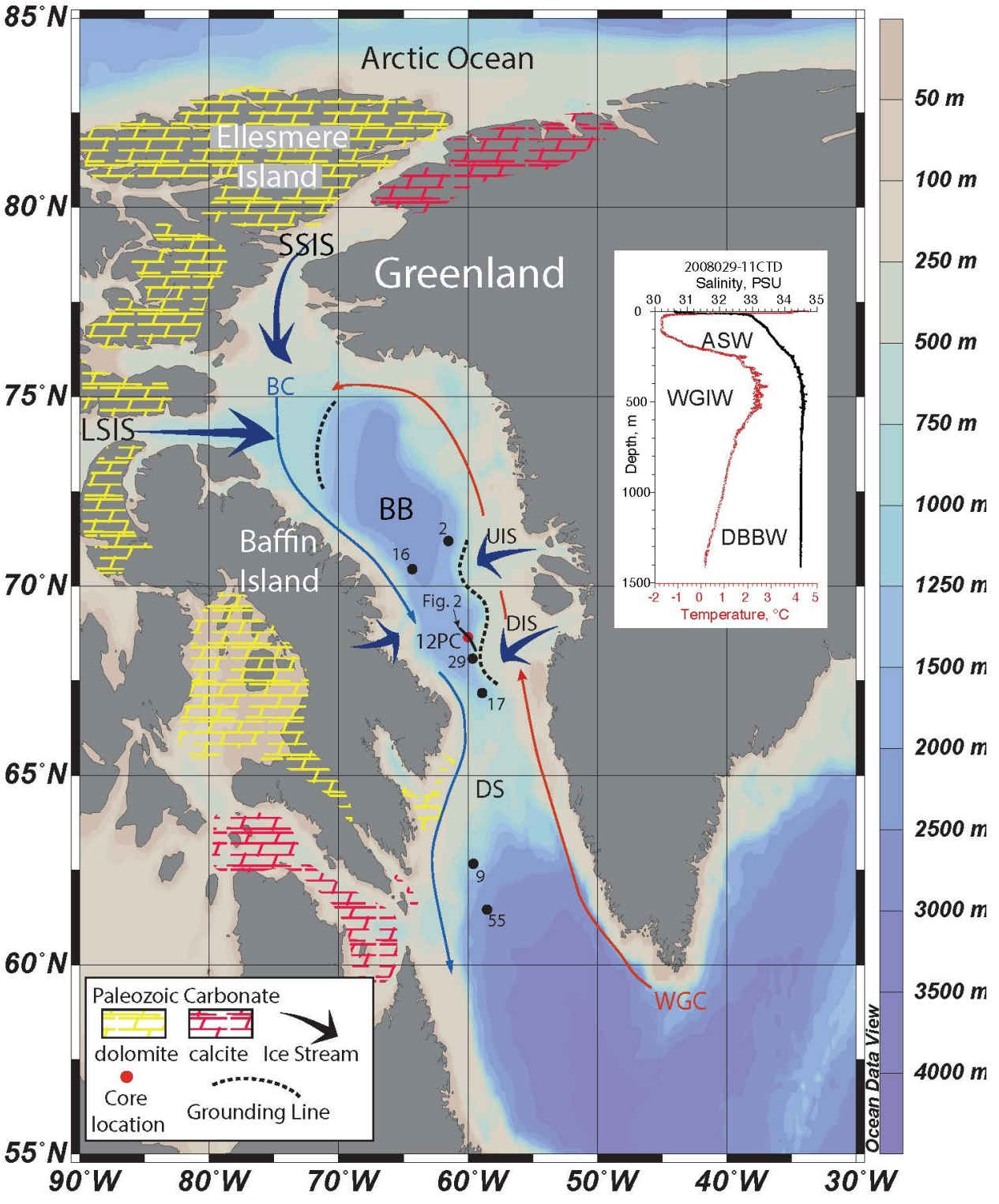

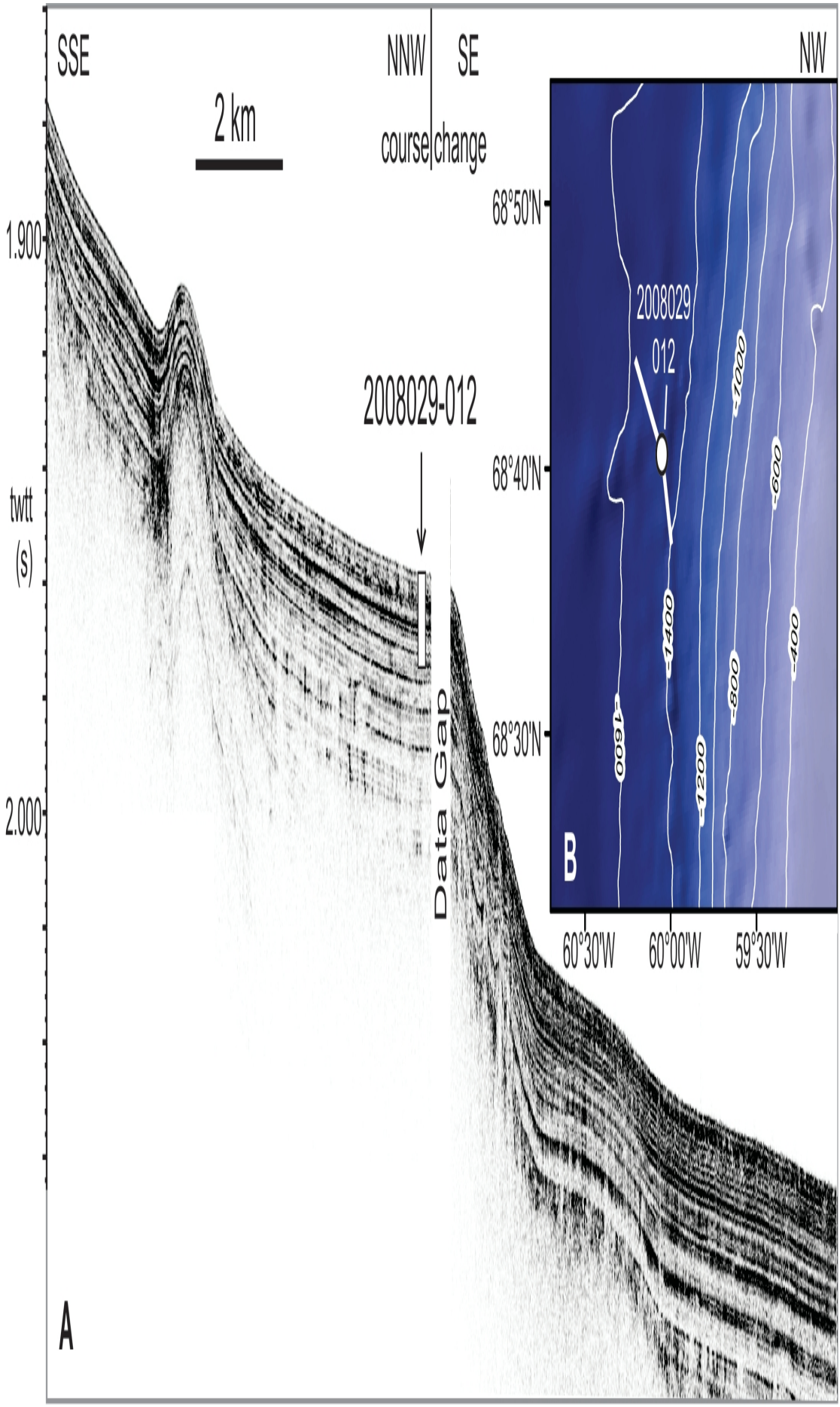

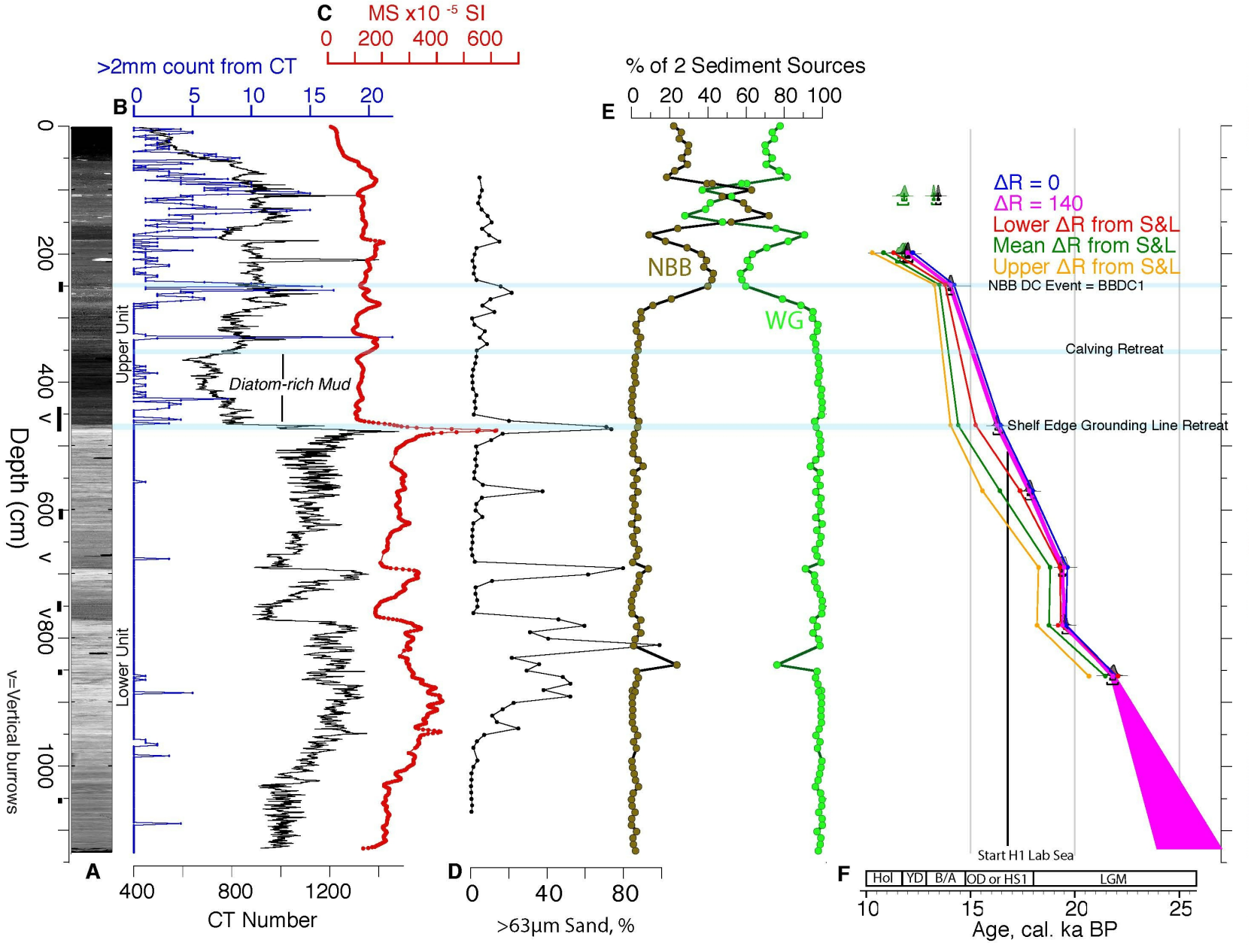

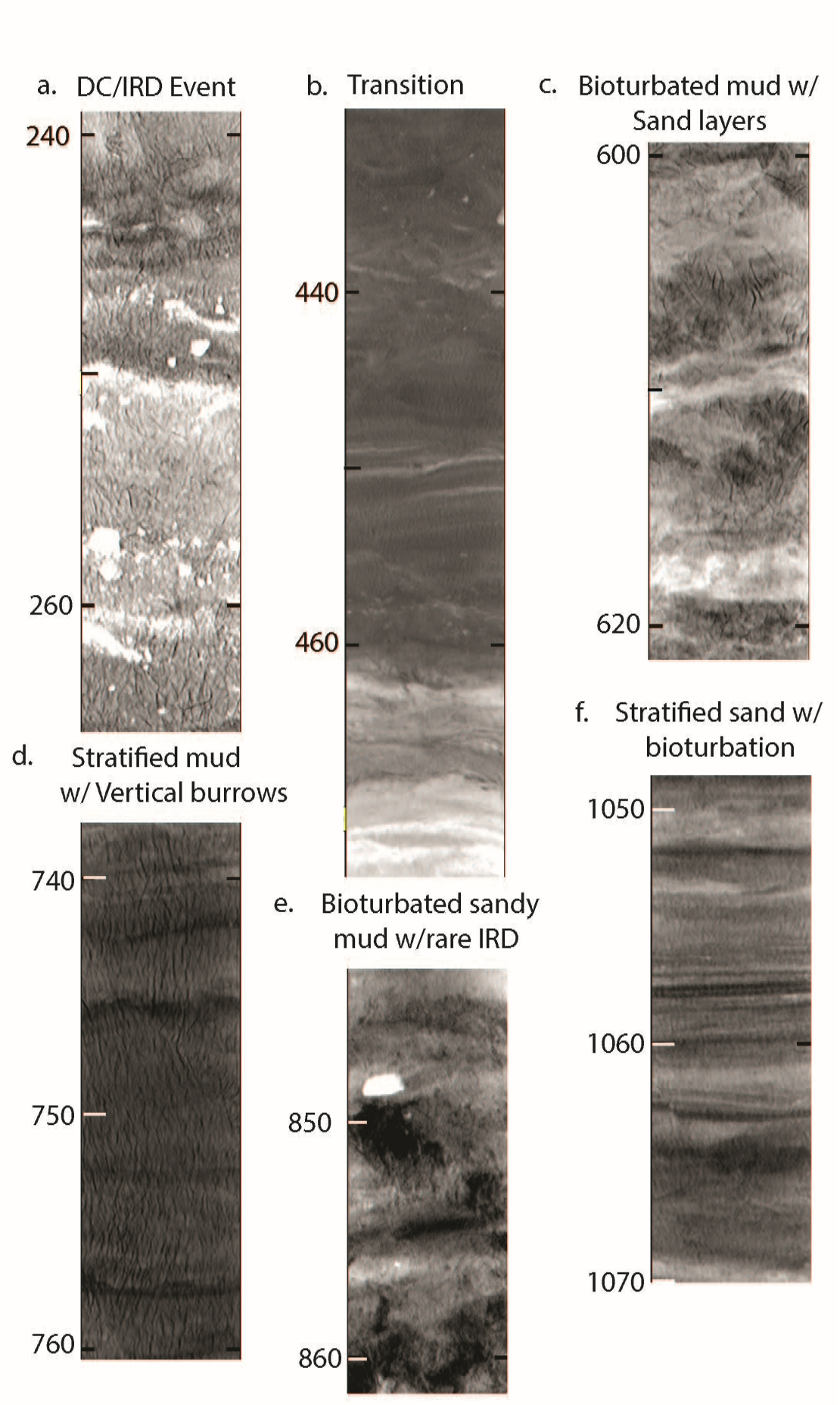

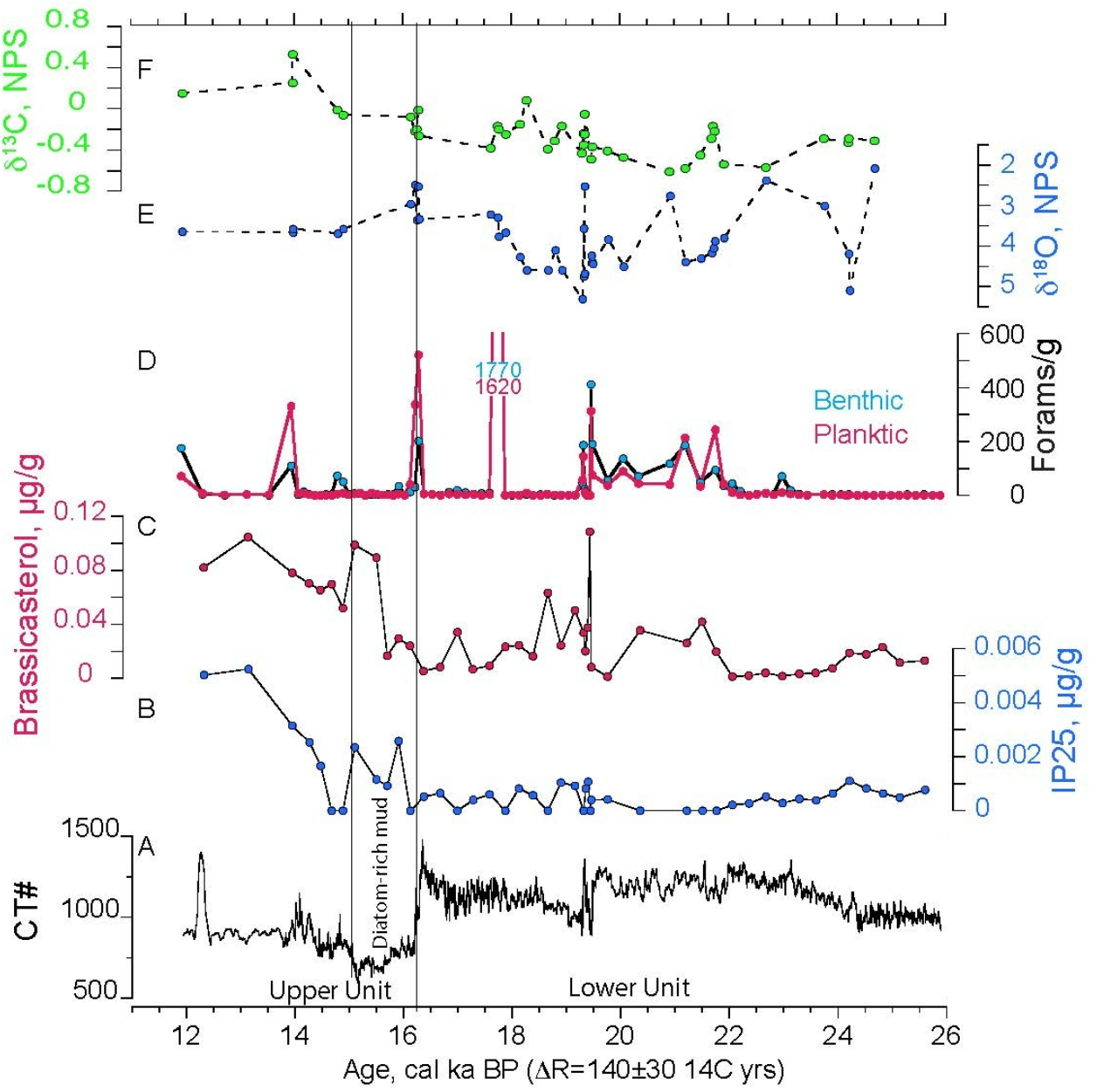

HU2008029-12PC Benthic Foraminifera

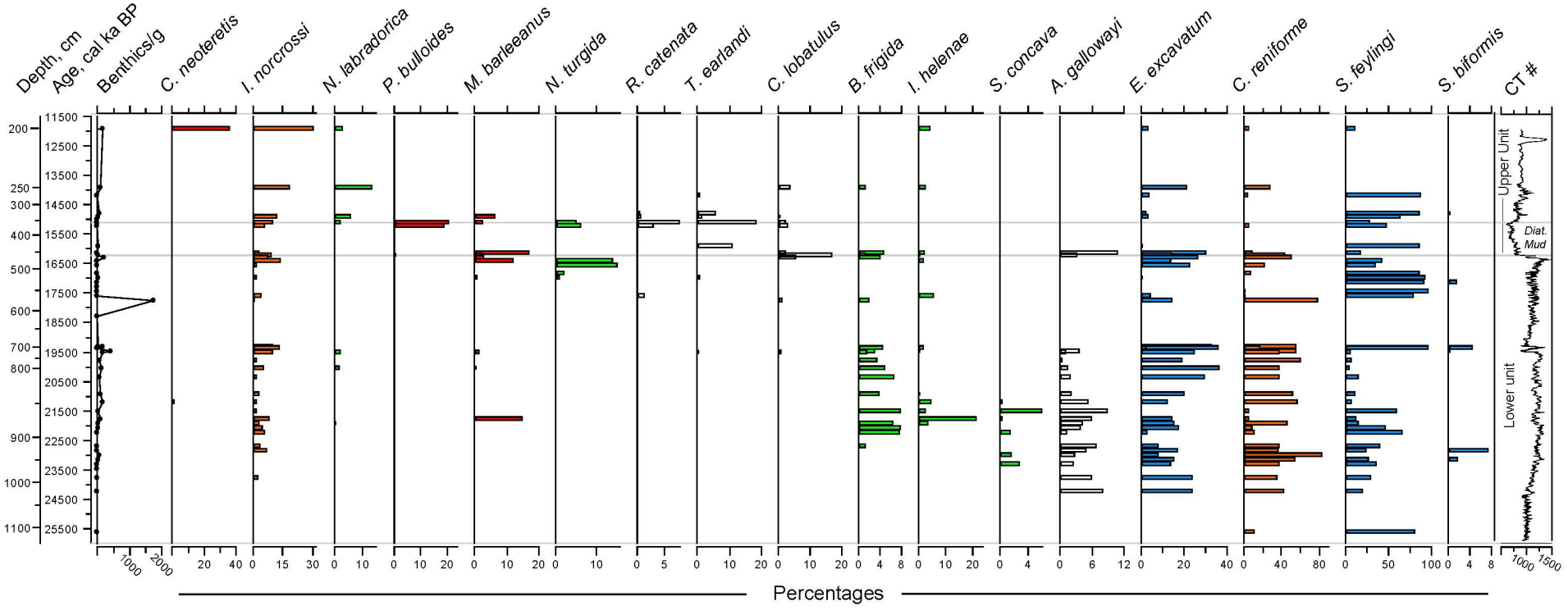

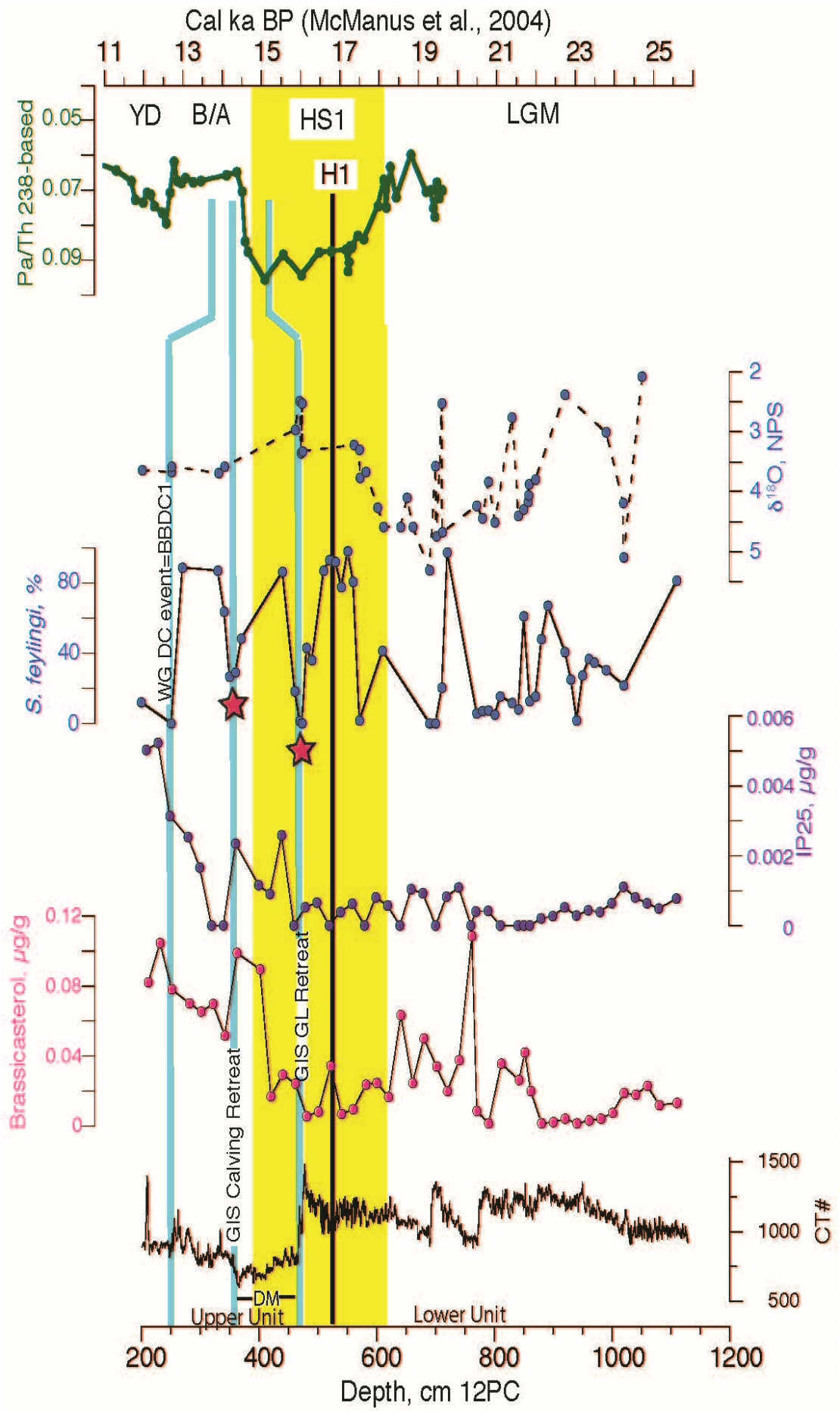

Table 1. Radiocarbon ages and their calibrations with varying ΔR.

Date	Depth	14C	error	ΔR	Date (14C ag
HU2008029-12PC					
CURL14065	201.5	10760	35	0	CURL14065 wi
CURL14065	201.5	10760	35	140	CURL14065 wi
CURL14065	201.5	10760	35	470	CURL14065 wi
CURL14065	201.5	10760	35	900	CURL14065 wi
CURL14065	201.5	10760	35	1340	CURL14065 wi
AA90386	251.5	12666	61	0	AA90386 with
AA90386	251.5	12666	61	140	AA90386 with
AA90386	251.5	12666	61	380	AA90386 with
AA90386	251.5	12666	61	630	AA90386 with
AA90386	251.5	12666	61	900	AA90386 with
CURL16671	469.5	14030	40	0	CURL16671 wi
CURL16671	469.5	14030	40	140	CURL16671 wi
CURL16671	469.5	14030	40	850	CURL16671 wi
CURL16671	469.5	14030	40	1260	CURL16671 wi
CURL16671	469.5	14030	40	1500	CURL16671 wi
CURL18165	571.5	15150	60	0	CURL18165 wi
CURL18165	571.5	15150	60	140	CURL18165 wi
CURL18165	571.5	15150	60	500	CURL18165 wi
CURL18165	571.5	15150	60	1150	CURL18165 wi
CURL18165	571.5	15150	60	1750	CURL18165 wi
CURL14067	690.5	16660	45	0	CURL14067 wi
CURL14067	690.5	16660	45	140	CURL14067 wi
CURL14067	690.5	16660	45	290	CURL14067 wi
CURL14067	690.5	16660	45	720	CURL14067 wi
CURL14067	690.5	16660	45	1250	CURL14067 wi
CURL16663	780.5	16600	50	0	CURL16663 wi
CURL16663	780.5	16600	50	140	CURL16663 wi
CURL16663	780.5	16600	50	290	CURL16663 wi
CURL16663	780.5	16600	50	720	CURL16663 wi
CURL16663	780.5	16600	50	1250	CURL16663 wi
CURL18628	859.5	18540	80	0	CURL18628 wi
CURL18628	859.5	18540	80	140	CURL18628 wi
CURL18628	859.5	18540	80	-50	CURL18628 wi
CURL18628	859.5	18540	80	420	CURL18628 wi
CURL18628	859.5	18540	80	1010	CURL18628 wi
Base of H1 ages from the Labrador Sea					
HU87033-009 LCF, 500-501 cm; Jennings et al., 1996					
AA-9364		14980	90	0	AA-9364 with
AA-9364		14980	90	140	AA-9364 with
AA-9364		14980	90	500	AA-9364 with

AA-9364	14980	90	1150	AA-9364 with
AA-9364	14980	90	1750	AA-9364 with
HU75009-IV-055PC, 115-117 cm; Kaufman and Williams, 1992				
AA-5999	15010	105	0	AA-5999 with
AA-5999	15010	105	140	AA-5999 with
AA-5999	15010	105	500	AA-5999 with
AA-5999	15010	105	1150	AA-5999 with
AA-5999	15010	105	1750	AA-5999 with

				Calibrated		
1sigma from	1sigma to	2sigma from	2sigma to	mean	error	
12306	12075	12430	12028	12215	109	
12026	11865	12100	11755	11937	86	
11317	11210	11432	11161	11282	70	
10868	10706	10972	10667	10805	79	
10291	10196	10373	10176	10260	51	
14279	14051	14542	13964	14208	142	
14095	13926	14165	13840	14007	83	
13845	13665	13930	13555	13748	91	
13552	13392	13657	13332	13484	81	
13312	13180	13375	13114	13246	66	
16511	16309	16632	16233	16423	102	
16311	16144	16424	16045	16232	90	
15282	15148	15375	15076	15221	73	
14507	14193	14701	14136	14398	155	
14086	13947	14143	13873	14011	68	
18035	17854	18130	17740	17941	94	
17887	17687	17973	17598	17785	97	
17465	17236	17549	17125	17345	110	
16491	16261	16631	16174	16390	117	
15680	15408	15776	15297	15541	128	
19698	19528	19832	19467	19631	91	
19550	19372	19609	19260	19449	88	
19368	19168	19466	19070	19268	99	
18850	18739	18905	18674	18791	57	
18328	18149	18395	18039	18226	90	
19634	19467	19749	19360	19553	91	
19480	19283	19560	19203	19380	93	
19257	19061	19385	18986	19177	99	
18802	18680	18856	18605	18735	62	
18267	18071	18337	17973	18160	94	
22113	21850	22271	21751	21993	131	
21916	21670	22057	21537	21795	127	
22175	21905	22301	21820	22051	128	
21594	21299	21746	21137	21442	149	
20772	20537	20913	20434	20662	119	
17878	17633	17984	17515	17752	120	
17725	17460	17883	17333	17599	136	
17281	16963	17437	16789	17115	161	

16288	16021	16449	15861	16155	140
15443	15143	15656	15041	15318	155
17916	17650	18037	17513	17780	133
17785	17490	17925	17345	17634	147
17345	17000	17495	16800	17156	174
16345	16032	16538	15875	16200	163
15528	15180	15733	15060	15367	174

median
12207
11943
11270
10796
10250
14180
14009
13751
13478
13246
16416
16230
15218
14378
14014
17943
17786
17349
16381
15544
19621
19455
19264
18793
18234
19551
19382
19173
18738
18163
21985
21798
22048
21444
20657
17753
17597
17115

16154
15302

17781
17633
17159
16195
15356